Available online at www.sciencedirect.com

SCIENCE DIRECT®

Coastal Engineering 51 (2004) 473–481

Coastal Engineering
An International Journal for Coastal, Harbour and Offshore Engineers

www.elsevier.com/locate/coastaleng

Effect of wave directional spread on the radiation stress: comparing theory and observations

Falk Feddersen

Center for Coastal Studies, Integrative Oceanography Division, Scripps Institution of Oceanography, University of California, San Diego, 9500 Gilman Dr., La Jolla, CA 92093-0209, USA

Received 15 May 2003; accepted 28 May 2004
Available online 3 August 2004

Abstract

Nearshore circulation and shoreline setup are forced through the wave radiation stress, which is a function of the frequency-directional wave spectrum. The radiation stress components often are approximated by assuming a spectrum that is narrow-band in frequency and direction. These narrow-band approximations overestimate the true radiation stress components in 8-m water depth on the Outer Banks, NC where locally generated (broad in frequency and direction) sea conditions are prevalent. Using the empirical Pierson-Moskowitz spectrum, frequency-spread is shown not to be the cause of this overestimation. Analytic expressions derived by Battjes [J. Mar. Res. 30 (1972) 56], for the ratio of true to narrow-band approximated radiation stress, which depend only on the directional spread, are compared to field data. The observed ratio of true to narrow-band approximated radiation stress is a strong function of the observed bulk (energy-weighted) directional spread, and closely follows the analytic expressions. Thus the narrow-band radiation stresses approximation can be augmented with a directional-spread dependence. These results are expected to apply to other geographic areas where waves are often locally generated.

Keywords: Nearshore environment; Ocean waves; Ocean currents; Surf zone

1. Introduction

Wave radiation stress gradients drive alongshore currents in the surf zone and lead to shoreline setup (Longuet-Higgins and Stewart, 1964; Bowen et al., 1968; Longuet-Higgins, 1970). Accurate offshore estimates of the radiation stress components S_{xy} and S_{xx} are required in alongshore current and setup models, respectively. The off-diagonal component S_{xy} in a directionally spread and frequency-spread (i.e., random) wave field is, according to linear theory (Battjes, 1972) (hereinafter $S^{(\mathrm{tr})}{}_{xy}$),

$$S_{xy} = \int_0^\infty \int_{-\pi}^{\pi} E(f,\theta)\frac{c_g(f)}{c(f)}\sin(\theta)\cos(\theta)\,\mathrm{d}\theta\mathrm{d}f, \quad (1)$$

where $E(f, \theta)$ is the frequency-directional $(f-\theta)$ energy spectrum, and $c_g(f)$ and $c(f)$ are the frequency dependent group and phase velocities, respectively. For a monochromatic (single frequency) and unidirec-

E-mail address: falk@coast.ucsd.edu (F. Feddersen).

0378-3839/$ - see front matter © 2004 Elsevier B.V. All rights reserved.
doi:10.1016/j.coastaleng.2004.05.008

tional (single wave angle) plane wave of height H, Eq. (1) reduces to

$$S_{xy} = \frac{1}{8}\rho g H^2 \frac{c_g}{c}\sin\theta\cos\theta, \tag{2}$$

where ρ is the water density, g is gravity, and c_g and c are evaluated at the monochromatic wave frequency.

For simplicity, alongshore current models that incorporate random waves (e.g., Church and Thornton, 1993; Ruessink et al., 2001) often assume that the wave spectrum is narrow banded in both frequency and direction, resulting in an approximation for $S_{xy}^{(nb)}$ similar to Eq. (2) (hereinafter $S_{xy}^{(nb)}$),

$$S_{xy}^{(nb)} = \frac{1}{8}\rho g H_{rms}^2 \frac{c_g(\bar{f})}{c(\bar{f})}\sin\bar{\theta}\cos\bar{\theta}, \tag{3}$$

where c_g and c are evaluated at the peak or mean (energy-weighted) wave frequency $\bar{f}$ and $\bar{\theta}$ is a peak or mean (energy-weighted) wave angle. The $S_{xy}^{(nb)}$ formulation (Eq. (3)) is appealing because it depends on a few components of the wave field.

The effect of directional spread on the radiation stress has been considered previously and mathematical expressions for corrections to the narrow-band approximations have been derived (Battjes, 1972). Using parameterized $E(f, \theta)$, Battjes (1972) showed that the narrow-band approximation can result in significant error in estimating S_{xy}. Indeed, in 8-m water depth at Duck, NC, the $S_{xy}^{(nb)}$ was consistently 60% larger than $S_{xy}^{(tr)}$ (Appendix A, Ruessink et al., 2001), which was suggested to result from directional spread of the wave field, but was not quantified. As discussed by Battjes (1972), errors in offshore S_{xy} will result in modeled alongshore current errors or, when fitting a model to observations, in biased alongshore current model parameters such as the drag coefficient.

The radiation stress component S_{xx} drives shoreline setup, and in a frequency- and directionally spread wave field, according to linear theory (Battjes, 1972), is (hereinafter $S_{xx}^{(tr)}$)

$$S_{xx} = \int_0^\infty \int_{-\pi}^{\pi} E(f,\theta) \times \left[\frac{c_g(f)}{c(f)}(\cos^2(\theta)+1) - \frac{1}{2}\right] d\theta df. \tag{4}$$

Similar to S_{xy}, the narrow-band in frequency and direction approximation to Eq. (4) is (hereinafter $S_{xx}^{(nb)}$)

$$S_{xx}^{(nb)} = \frac{1}{8}\rho g H_{rms}^2 \left[\frac{c_g(\bar{f})}{c(\bar{f})}(\cos^2(\bar{\theta})+1) - \frac{1}{2}\right]. \tag{5}$$

This $S_{xx}^{(nb)}$ or other simplifications (e.g., zero directional-spread, shallow-water, and $\bar{\theta}=0$) often are used in studies of the cross-shore momentum (i.e., setup) balances (e.g., Guza and Thornton, 1981; Nielsen, 1988; King et al., 1990; Lentz and Raubenheimer, 1999; Lentz et al., 1999; Raubenheimer et al., 2001). As discussed by Battjes (1972), the narrow-band $S_{xx}^{(nb)}$ may over- or underestimate the true $S_{xx}^{(tr)}$, resulting in over- or underestimated setup. Although, it is noted that Raubenheimer et al. (2001) found small differences in setup predictions using $S_{xx}^{(tr)}$ or $S_{xx}^{(nb)}$.

In principle a directional wave buoy or current-meter provides the information required to estimate $S_{xy}^{(tr)}$ and $S_{xx}^{(tr)}$ (e.g., Longuet-Higgins et al., 1963; Higgins et al., 1981; Elgar et al., 1994), although this capability is not always utilized. Here, the true and narrow-band S_{xy} and S_{xx} formulations are examined. In 8-m water depth, the narrow-band $S_{xy}^{(nb)}$ and $S_{xx}^{(nb)}$ are consistently larger (by 60% and 16%, respectively) than the true $S_{xy}^{(tr)}$ and $S_{xx}^{(tr)}$. The breakdown of the narrow-band approximation is examined by separately studying the effects of frequency and directional spread. Using an empirical frequency spectrum, the effect of frequency spread is shown to be small and unlikely to explain the error in the narrow-band approximation. Assuming zero frequency-spread and symmetric directional spectra, analytic expressions (Battjes, 1972) for the $S_{xy}^{(tr)}/S_{xy}^{(nb)}$ and $S_{xx}^{(tr)}/S_{xx}^{(nb)}$ ratios are functions of the directional spread. The observed ratios are strong functions of the observed directional spread and the analytic expressions reproduce this dependence, demonstrating that the true $S_{xy}^{(tr)}$ and $S_{xx}^{(tr)}$ can be accurately parameterized by augmenting the $S_{xy}^{(nb)}$ and $S_{xx}^{(nb)}$ representations with a directional-spread dependence.

2. Observations

Wave observations were taken near Duck, NC on the northern part of the Outer Banks in the mid-

Atlantic Bight with a pressure sensor array in 8-m water depth (Long, 1996) maintained by the U.S. Army Corps of Engineers Field Research Facility during the Duck94 (August–October 1994) and the SandyDuck (August–November 1997) field experiments. Hourly $S_{xy}^{(\mathrm{tr})}$ and $S_{xx}^{(\mathrm{tr})}$ were calculated using a moment-estimation technique (Elgar et al., 1994), and hourly rms wave height H_{rms}, bulk (energy-weighted) mean angle $\bar{\theta}$, and frequency $\bar{f}$ (Appendix A) were used to the calculate narrow-band approximations $S_{xy}^{(\mathrm{nb})}$ (Eq. (3)) and $S_{xx}^{(\mathrm{nb})}$ (Eq. (5)). Additionally, bulk (energy-weighted) directional spread $\bar{\sigma}_{\theta}$ (Eq. (A2)) (Kuik et al., 1988) was calculated (Appendix A). A total of 2202 and 2635 hourly estimates were collected for Duck94 and SandyDuck, respectively. A wide range of wave conditions occurred in 8-m water depth (Table 1), with the average condition being a locally generated sea typical of the mid-Atlantic Bight.

As noted by Ruessink et al. (2001) for Duck94, during both experiments the $S_{xy}^{(\mathrm{tr})}$ and $S_{xy}^{(\mathrm{nb})}$ estimates are correlated ($r=0.98$), but the narrow-band $S_{xy}^{(\mathrm{nb})}$ is consistently larger than the true $S_{xy}^{(\mathrm{tr})}$ (Fig. 1a and b). The best-fit slopes (0.63) are nearly identical for the two experiments, and indicate a systematic 60% overestimation of S_{xy} by using $S_{xy}^{(\mathrm{nb})}$. This overestimation with the narrow-band approximation applies also to S_{xx} (Fig. 2). The Duck94 and SandyDuck true $S_{xx}^{(\mathrm{tr})}$ and narrow-band $S_{xx}^{(\mathrm{nb})}$ are correlated ($r=0.99$), but the narrow-band $S_{xx}^{(\mathrm{nb})}$ is consistently larger than $S_{xx}^{(\mathrm{tr})}$ with similar best-fit slopes (Duck94: 0.86 and SandyDuck: 0.89). Use of the narrow-band $S_{xx}^{(\mathrm{nb})}$ would result in overpredicted modeled shoreline setup.

Thornton and Guza (1986) recognized the potential error in using $S_{xy}^{(\mathrm{nb})}$. They drove an alongshore current model with an S_{xy} conserving wave angle $\hat{\theta}$ (Higgins et al., 1981) defined so that, in

Table 1
Combined Duck94 and SandyDuck hourly wave statistics in 8-m water depth

	H_{rms} (m)	$\bar{f}$ (Hz)	$\lvert\bar{\theta}\rvert$ (deg)	$\bar{\sigma}_{\theta}$ (deg)
Mean	0.58	0.15	16	23
Standard deviation	0.39	0.03	11	4
Maximum	2.88	0.25	58	45
Minimum	0.12	0.08	0	13

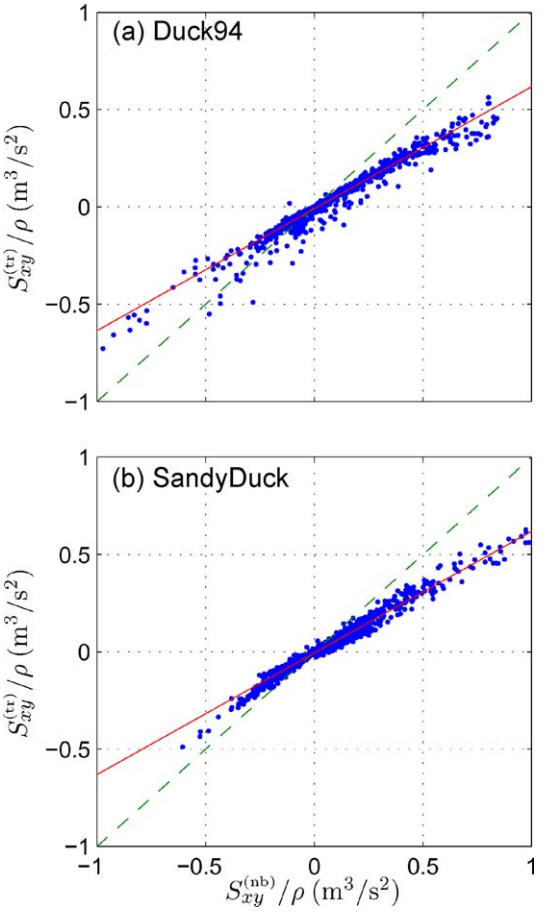

Fig. 1. (a) Duck94 and (b) SandyDuck true $S_{xy}^{(\mathrm{tr})}/\rho$ vs. narrow-band $S_{xy}^{(\mathrm{nb})}/\rho$. The dashed line is the one-to-one relationship. The correlation for both is $r=0.98$ and the best-fit slopes (solid lines) are both 0.63. Positive S_{xy} corresponds to waves from the north.

9-m water depth at a beach near Santa Barbara, CA,

$$\frac{1}{8}\rho g H_{\mathrm{rms}}^2 \frac{c_g(\bar{f})}{c(\bar{f})}\sin\hat{\theta}\cos\hat{\theta} = S_{xy}^{(\mathrm{tr})},$$

where the peak frequency of the spectrum was used for $\bar{f}$ and $S_{xy}^{(\mathrm{tr})}$ was calculated with an array of pressure sensors. Small differences (0.2–2.7°) were found between $\hat{\theta}$ and the mean angle at the peak frequency (analogous to $\bar{\theta}$). Perhaps this agreement led to a more general adoption of the narrow-band $S_{xy}^{(\mathrm{nb})}$ approximation (Eq. (3)). However, Thornton and Guza (1986) observed very long period ocean swell, and thus the narrow-band (for both f and θ) approximations were

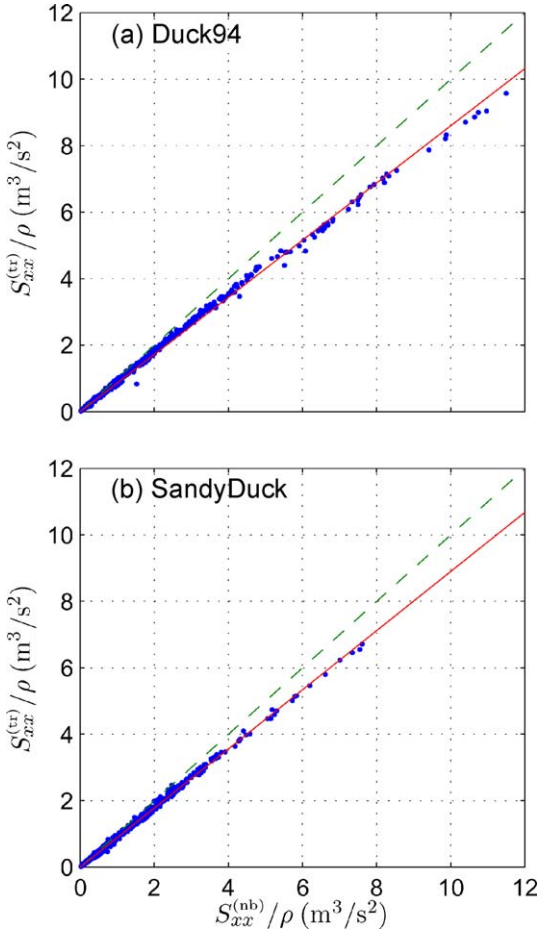

Fig. 2. (a) Duck94 and (b) SandyDuck true $S_{xx}^{(tr)}/\rho$ vs. narrow-band $S_{xx}^{(nb)}/\rho$. The dashed line is the one-to-one relationship. The correlation for both is $r=0.99$ and the best-fit slopes (solid lines) are 0.86 and 0.89, respectively.

likely satisfied. In contrast, the Duck wave field is often locally generated, with a broad frequency-directional spectrum, resulting in typical 10–20° differences between $\bar{\theta}$ and $\hat{\theta}$ (not shown). Analogous differences occur with an S_{xx} conserving angle.

3. Radiation stress parameterizations

The breakdown of the narrow-band approximation is examined by considering a separable frequency-directional spectrum, i.e.,

$$E(f,\theta) = F(f)D(\theta-\bar{\theta}), \tag{6}$$

where $D(\theta-\bar{\theta})$ is normalized so that $\int_{-\pi}^{\pi} D(\theta-\bar{\theta})\mathrm{d}\theta = 1$ and $\int_0^\infty F(f)\mathrm{d}f = E_0$ where E_0 is the total wave energy (i.e., $E_0=\rho g H_{\mathrm{rms}}^2/8$). Although real oceanic $E(f,\theta)$ are rarely separable, this provides a springboard to examine separately the effects of frequency-spread and directional-spread on S_{xy} and S_{xx}. With Eq. (6), the expressions for $S_{xy}^{(tr)}$ and $S_{xx}^{(tr)}$ become,

$$S_{xy}^{(tr)} = \int_0^\infty F(f)\frac{c_g(f)}{c(f)}\mathrm{d}f \times \int_{-\pi}^{\pi} D(\theta-\bar{\theta})\sin(\theta)\cos(\theta)\,\mathrm{d}\theta \tag{7a}$$

$$S_{xx}^{(tr)} = \int_0^\infty F(f)\frac{c_g(f)}{c(f)}\mathrm{d}f \times \left[1+\int_{-\pi}^{\pi} D(\theta-\bar{\theta})\cos^2(\theta)\mathrm{d}\theta\right] - \frac{1}{2}E_0. \tag{7b}$$

3.1. Frequency spread

Frequency-spread results in variable c_g/c which in intermediate water depths could potentially affect the radiation stress. For example, in 8-m water depth, c_g/c spans 0.66–0.95 over the frequency range 0.07–0.2 Hz. To isolate frequency spread effects, consider a narrow-banded directional spectrum $E(f,\theta)=F(f)\delta(\theta-\bar{\theta})$ where δ is a Dirac delta function. The expressions for $S_{xy}^{(tr)}$ (Eq. (7a)) and $S_{xx}^{(tr)}$ (Eq. (7b)) become

$$S_{xy}^{(tr)} = \int_0^\infty F(f)\frac{c_g(f)}{c(f)}df \times \sin(\bar{\theta})\cos(\bar{\theta}),$$

$$S_{xx}^{(tr)} = \int_0^\infty F(f)\frac{c_g(f)}{c(f)}df \times [1+\cos^2(\bar{\theta})] - \frac{1}{2}E_0.$$

The amount the frequency-spread contributes to error in $S_{xy}^{(nb)}$ and $S_{xx}^{(nb)}$ is given by the ratios

$$\frac{S_{xy}^{(tr)}}{S_{xy}^{(nb)}} = \frac{\int_0^\infty F(f)\frac{c_g(f)}{c(f)}\mathrm{d}f}{E_0\frac{c_g(\bar{f})}{c(\bar{f})}}, \tag{8a}$$

$$\frac{S_{xx}^{(tr)}}{S_{xx}^{(nb)}} = \frac{\int_0^\infty F(f)\frac{c_g(f)}{c(f)}df \times [1+\cos^2(\bar{\theta})] - \frac{1}{2}\mathrm{E}_0}{E_0\left[\frac{c_g(\bar{f})}{c(\bar{f})}(1+\cos^2(\bar{\theta})) - \frac{1}{2}\right]}. \tag{8b}$$

Although the possible permutations of oceanic $F(f)$ are limitless, for analysis purposes a Pierson and Moskowitz (1964, hereinafter PM) spectrum is considered

$$F_{\mathrm{PM}}(f) = \frac{\alpha g^2 f^{-5}}{(2\pi)^4}\exp\left[-\frac{5}{4}\left(\frac{f}{f_\mathrm{p}}\right)^{-4}\right]$$

where f_p is the peak frequency, g represents gravity, and α sets the total wave energy. Note that there is a difference between the peak frequency f_p and the energy-weighted mean frequency $\bar{f}$ ($\bar{f}=1.25^{1/4}\Gamma(3/4)f_\mathrm{p} \approx 1.3f_\mathrm{p}$). Although the PM spectrum is intended for deep-water waves, it is not much different from empirical finite-depth spectral forms (e.g., Bouws et al., 1985), and is useful because it has one free parameter f_p. The $S_{xy}^{(\mathrm{tr})}/S_{xy}^{(\mathrm{nb})}$ and $S_{xx}^{(\mathrm{tr})}/S_{xx}^{(\mathrm{nb})}$ ratios (Eqs. (8a) and (8b)) with the PM spectrum are efficiently numerically integrated (Abramowitz and Stegun, 1965) and are functions soley of $\bar{f}$.

3.2. Directional spread

In examining the effects of directional spread, the analysis of Battjes (1972) is followed. With frequency spectrum $F(f)=E_0\delta(f-\bar{f})$ and symmetric $D(\theta-\bar{\theta})$, The expression for $S_{xy}^{(\mathrm{tr})}$ (Eq. (7a)) becomes (with $\theta'=\theta-\bar{\theta}$)

$$S_{xy}^{(\mathrm{tr})} = E_0\frac{c_\mathrm{g}(\bar{f})}{c(\bar{f})}\sin(\bar{\theta})\cos(\bar{\theta})\underbrace{\int_{-\pi}^{\pi} D(\theta')\cos(2\theta')\mathrm{d}\theta'}_{R}.$$

The theta-integral R is the ratio $S_{xy}^{(\mathrm{tr})}/S_{xy}^{(\mathrm{nb})}$ which is ≤ 1, and using circular moment definitions reduces to (Battjes, 1972)

$$\frac{S_{xy}^{(\mathrm{tr})}}{S_{xy}^{(\mathrm{nb})}} = 1 - 2\sigma_\theta^{*2}, \tag{9}$$

where σ_θ^* is the directional-spread[1] (Kuik et al., 1988). The expression for $S_{xx}^{(\mathrm{tr})}$ (Eq. (7b)) becomes

$$S_{xx}^{(\mathrm{tr})} = E_0\left[\frac{c_\mathrm{g}(\bar{f})}{c(\bar{f})}\left(1+\underbrace{\int_{-\pi}^{\pi} D(\theta-\bar{\theta})\cos^2(\theta)\mathrm{d}\theta}_{S}\right) - \frac{1}{2}\right] \tag{10}$$

The theta integral S in Eq. (10) reduces to

$$\begin{aligned}\int_{-\pi}^{\pi} D(\theta-\bar{\theta})\cos^2(\theta)\mathrm{d}\theta &= \cos^2(\bar{\theta})\int_{-\pi}^{\pi} D(\theta')\cos^2(\theta')\mathrm{d}\theta' \\ &\quad + \sin^2(\bar{\theta})\int_{-\pi}^{\pi} D(\theta')\sin^2(\theta')\mathrm{d}\theta' \\ &= \cos^2(\bar{\theta})(1-\sigma_\theta^{*2}) + \sin^2(\bar{\theta})\sigma_\theta^{*2}.\end{aligned} \tag{11}$$

The second term in Eq. (11) is often negligible relative to the first term. For example, with even large $\bar{\theta}=30^\circ$ and $\sigma_\theta^*=30^\circ$ values (Table 1), the second term is only 13% of the first. Neglecting the second term, the $S_{xx}^{(\mathrm{tr})}/S_{xx}^{(\mathrm{nb})}$ ratio becomes (analogous to the deep water result in Battjes (1972))

$$\frac{S_{xx}^{(\mathrm{tr})}}{S_{xx}^{(\mathrm{nb})}} = \frac{\frac{c_\mathrm{g}}{c}[(1-\sigma_\theta{}^{*2})\cos^2(\bar{\theta})+1] - \frac{1}{2}}{\frac{c_\mathrm{g}}{c}[\cos^2(\bar{\theta})+1] - \frac{1}{2}},$$

and assuming small angles ($\cos\bar{\theta}\approx 1$) and shallow water waves ($c_g/c \approx 1$), the ratio reduces to

$$\frac{S_{xx}^{(\mathrm{tr})}}{S_{xx}^{(\mathrm{nb})}} = 1 - \frac{2}{3}\sigma_\theta^{*2}. \tag{12}$$

4. Results

Although oceanic $E(f,\theta)$ are not in general separable and θ symmetric, the combined Duck94 and SandyDuck observed $S_{xy}^{(\mathrm{tr})}/S_{xy}^{(\mathrm{nb})}$ and $S_{xx}^{(\mathrm{tr})}/S_{xx}^{(\mathrm{nb})}$ are examined to determine whether frequency or directional spread can explain the systematic difference between

[1] Kuik et al. (1988) defines two directional spreads: $\sigma_\theta^{*2} = \int_{-\pi}^{\pi}\sin^2(\theta')D(\theta')\mathrm{d}\theta'$ and $\sigma_\theta^2 = 4\int_{-\pi}^{\pi}\sin^2(\theta'/2)D(\theta')\mathrm{d}\theta'$.

the true and narrow-band radiation stress representations (Figs. 1 and 2). Both $S_{xx}^{(tr)}/S_{xy}^{(nb)}$ and $S_{xx}^{(tr)}/S_{xx}^{(nb)}$ are binned as functions of the observed (Appendix A) $\bar{f}$ and bulk (energy-weighted) $\bar{\sigma}_\theta^*$ (Eq. (A2)) from which means and standard deviations are calculated. Binned observations are restricted ($|S_{xy}^{(nb)}| \geq 0.06$ m^3/s^2 and $|\bar{\theta}| \geq 5°$, and $S_{xx}^{(nb)}/\rho \geq 0.8$ m^3/s^2) so that ratios are not biased by dividing by exceedingly small numbers. This corresponds to excluding cases with very small waves that are not of typical interest. Changing these restrictions does not change the results. The integral expressions for $S_{xy}^{(tr)}/S_{xy}^{(nb)}$ and $S_{xx}^{(tr)}/S_{xx}^{(nb)}$ based solely on frequency-spread (Eqs. (8a) and (8b)) using the PM spectrum are calculated with 8-m water depth and $\bar{\theta}=0$. Varying the depth between 5 and 13 m and $\bar{\theta}$ by 20° does not change the ratios significantly. The analytic $S_{xy}^{(tr)}/S_{xy}^{(nb)}$ and $S_{xx}^{(tr)}/S_{xx}^{(nb)}$ $S_{xx}^{(nb)}$ based solely on directional spread (Eqs. 9 and 12) are calculated as a function of the bulk $\bar{\sigma}_\theta^*$.

The effects of frequency spread are examined first (Fig. 3). The observed $S_{xy}^{(tr)}/S_{xy}^{(nb)}$ means range between 0.55 and 0.8, with standard deviations about 0.15 (Fig. 3a). The observed $S_{xx}^{(tr)}/S_{xx}^{(nb)}$ means (between 0.85 and 0.95) do not strongly vary with $\bar{f}$ (Fig. 3b). The PM based numerically integrated $S_{xy}^{(tr)}/S_{xy}^{(nb)}$ and $S_{xx}^{(tr)}/S_{xx}^{(nb)}$ are near 1 (dash-dot curves in Fig. 3), and, in contrast to the observed ratios, increases (slightly) with larger $\bar{f}$. At $\bar{f}$>0.2 Hz, the PM based numerically integrated maximum ratios are $S_{xy}^{(tr)}/S_{xy}^{(nb)}=1.08$ and $S_{xx}^{(tr)}/S_{xx}^{(nb)}=1.15$. Thus, for a PM spectrum, frequency spread is unable to explain the observed $S_{xy}^{(tr)}/S_{xy}^{(nb)}$ and $S_{xx}^{(tr)}/S_{xx}^{(nb)}$ ratios, and although the PM spectrum is by no means universal—particularly in intermediate depths, this strongly suggests that frequency spread is not the cause of the observed $S_{xy}^{(tr)}/S_{xy}^{(nb)}$ and $S_{xx}^{(tr)}/S_{xx}^{(nb)}$.

The effect of directional-spread are examined next with the bulk (energy-weighted) $\bar{\sigma}_\theta^*$ (Eq. (A2)) used in the place of the single wave frequency $\bar{\sigma}_\theta^*$. The $S_{xy}^{(tr)}/S_{xy}^{(nb)}$ and $S_{xx}^{(tr)}/S_{xx}^{(nb)}$ ratios both are strong functions $\bar{\sigma}_\theta^*$ (Fig. 4). The $S_{xy}^{(tr)}/S_{xy}^{(nb)}$ binned means range between 0.32 and 0.82 closely following the analytical expression of Battjes (1972) (Eq. (9)). Most binned standard deviations are ≤ 0.1 (Fig. 4a) indicating little scatter. At the mean $\bar{\sigma}_\theta^*=23°$ (Table 1) the analytic $S_{xy}^{(tr)}/S_{xy}^{(nb)}=0.66$, close to the best-fit value of 0.63 (light dashed line in Fig. 4a). The $S_{xx}^{(tr)}/S_{xx}^{(nb)}$ binned means range between 0.78 and 0.94

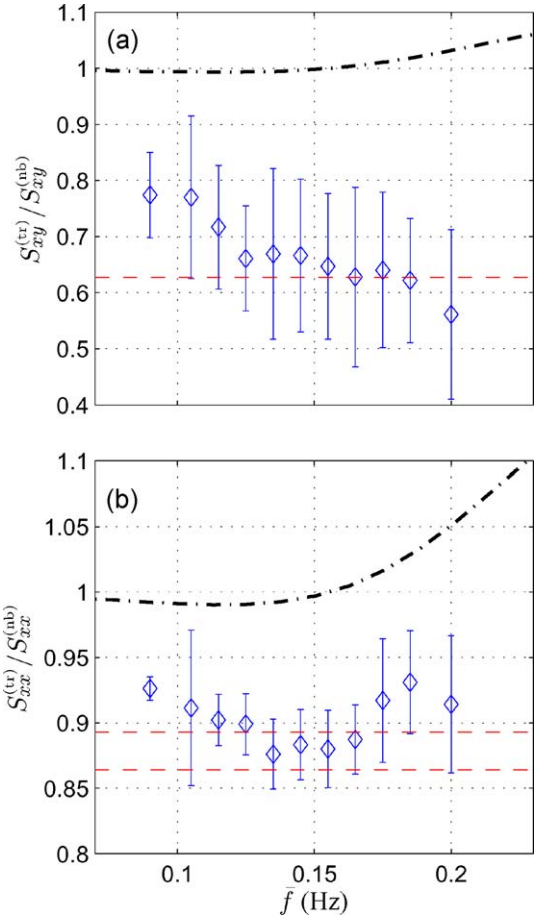

Fig. 3. Combined Duck94 and SandyDuck means (diamonds) and standard deviations (vertical bars) of (a) $S_{xy}^{(tr)}/S_{xy}^{(nb)}$ and (b) $S_{xx}^{(tr)}/S_{xx}^{(nb)}$ vs. mean frequency $\bar{f}$. The dash-dot curves represent the effects of frequency-spread (Eqs. (8a) and (8b)) using the Pierson and Moskowitz (1964) spectrum. The horizontal dashed lines in panels a and b represent the best fit slopes in Figs. 1 and 2, respectively.

also closely following the analytic expression (Eq. (12)), and have standard deviations ≤ 0.06. The observed best-fit slopes from Fig. 2 (0.86 and 0.89, light dashed lines in Fig. 4b) intersect the analytic curve within the observed $\bar{\sigma}_\theta^*$ mean ± one standard deviation (23 ± 4°). This demonstrates that the observed difference between the true and narrow-band radiation stresses is due to directional spread of the incident wave field, and shows that the true $S_{xy}^{(tr)}$ and $S_{xx}^{(tr)}$ can be accurately parameterized given the bulk wave parameters H_{rms}, $\bar{f}$, $\bar{\theta}$, and $\bar{\sigma}_\theta^*$.

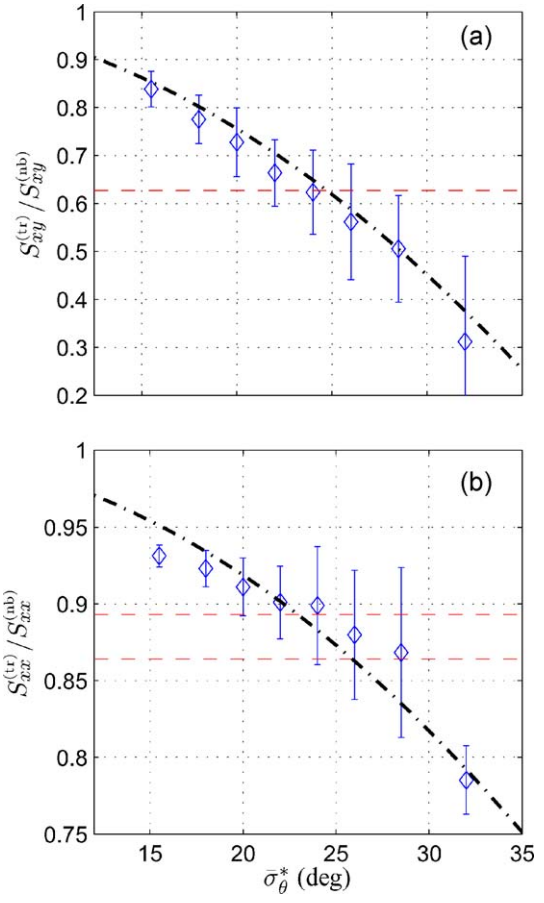

Fig. 4. Combined Duck94 and SandyDuck means (diamonds) and standard deviations (vertical bars) of (a) $S_{xy}^{(tr)}/S_{xy}^{(nb)}$ and (b) $S_{xx}^{(tr)}/S_{xx}^{(nb)}$ vs. $\bar{\sigma}_\theta^*$. The dash-dot curves represent the analytic $S_{xy}^{(tr)}/S_{xy}^{(nb)}$ and $S_{xx}^{(tr)}/S_{xx}^{(nb)}$ dependence of $\bar{\sigma}_\theta^*$ (Eqs. (9) and (12)). The horizontal dashed lines in panels a and b represent the best fit slopes in Figs. 1 and 2, respectively.

The directional spread decreases due to refraction as waves propagate toward shore. For zero frequency spread and small directional spread, the cross-shore (x) transformation of $\bar{\sigma}_\theta^*$ due to Snell's law is (Kinsman, 1965)

$$\frac{\bar{\sigma}_\theta^*(x)}{\bar{\sigma}_\theta^*(x_0)} = \frac{c(x)}{c(x_0)} \frac{\cos[\bar{\theta}(x_0)]}{\cos[\bar{\theta}(x)]}$$

where x_0 is an offshore location. Given the observed mean $\bar{f} = 0.15$ Hz and $\bar{\theta} = 16°$ (Table 1), the directional-spread in 3-m water depth is still 2/3 the 8-m depth $\bar{\sigma}_\theta^*$. Furthermore with wave-breaking, $\bar{\sigma}_\theta^*$ can increase up to 50% and reach values up to 30° (Herbers et al., 1999). Thus, the results in 8-m depth appear to be relevant in shallower water.

5. Summary

The narrow-band (in frequency and direction) approximation to the radiation stress ($S_{xy}^{(nb)}$ and $S_{xx}^{(nb)}$) often is used in modeling the alongshore currents and setup. However, in 8-m water depth at Duck, NC the narrow-band approximated radiation stress components are systematically larger than the true radiation stress components ($S_{xy}^{(tr)}$ and $S_{xx}^{(tr)}$) based on moments of the frequency-directional spectrum. Clearly, the true radiation stress, which can be estimated from a current meter or directional wave buoy, should be used whenever possible. Use of the narrow band radiation stress approximations will result in biased alongshore current and shoreline setup, or result in biased alongshore current model parameters when fitting models to observations. This difference between the narrow band and true radiation stress is not the result of frequency-spread, but is due to nonzero directional spread (Battjes, 1972).

Assuming a narrow-frequency, directionally symmetric frequency-directional spectrum leads to analytic expressions for the $S_{xy}^{(tr)}/S_{xy}^{(nb)}$ and $S_{xx}^{(tr)}/S_{xx}^{(nb)}$ ratios that accurately describe the observed ratios with the bulk $\bar{\sigma}_\theta^*$. While these results are presented for only a single geographic location and one water depth, observations total 7 months, and it is expected that these results are valid for other geographic locations where the waves are often locally generated.

Acknowledgements

This research was supported by NOPP and WHOI. The Field Research Facility, Coastal Engineering Research Center, Duck, NC provided the 8-m depth pressure array data, processed by Tom Herbers. Bob Guza, John Trowbridge, and Jurgen Battjes provided valuable feedback.

Appendix A. Definition of energy-weighted wave statistics

The mean frequency $\bar{f}$ is defined as

$$\bar{f} = \frac{\int_{ss}\int_{-\pi}^{\pi} f E(f,\theta)\mathrm{d}\theta\ \mathrm{d}f}{\int_{ss}\int_{-\pi}^{\pi} f E(f,\theta)\mathrm{d}\theta\ \mathrm{d}f}$$

where the frequency integral is over the sea-swell (ss) frequency band (0.044–0.3 Hz).

Directional moments, defined by Kuik et al. (1988) at a single frequency, are generalized for the entire sea-swell frequency band. With the lowest four bulk Fourier directional-moments of $E(f,\theta)$ (Longuet-Higgins et al., 1963; Herbers et al., 1999),

$$a_1 = \frac{\int_{ss}\int_{-\pi}^{\pi} \cos(\theta)E(f,\theta)\mathrm{d}\theta\ \mathrm{d}f}{\int_{ss}\int_{-\pi}^{\pi} E(f,\theta)\mathrm{d}\theta\ \mathrm{d}f},$$

$$b_1 = \frac{\int_{ss}\int_{-\pi}^{\pi} \sin(\theta)E(f,\theta)\mathrm{d}\theta\ \mathrm{d}f}{\int_{ss}\int_{-\pi}^{\pi} E(f,\theta)\mathrm{d}\theta\ \mathrm{d}f},$$

$$a_2 = \frac{\int_{ss}\int_{-\pi}^{\pi} \cos(2\theta)E(f,\theta)\mathrm{d}\theta\ \mathrm{d}f}{\int_{ss}\int_{-\pi}^{\pi} E(f,\theta)\mathrm{d}\theta\ \mathrm{d}f},$$

$$b_2 = \frac{\int_{ss}\int_{-\pi}^{\pi} \sin(2\theta)E(f,\theta)\mathrm{d}\theta\ \mathrm{d}f}{\int_{ss}\int_{-\pi}^{\pi} E(f,\theta)\mathrm{d}\theta\ \mathrm{d}f}.$$

the energy-weighted mean wave angle $\bar{\theta}$ and directional spread $\bar{\sigma}_\theta^*$ are defined as (Kuik et al., 1988),

$$\bar{\theta} = \arctan(b_1/a_1),$$

$$(\bar{\sigma}_\theta^*)^2 = \frac{1 - a_2\cos(2\bar{\theta}) - b_2\sin(2\bar{\theta})}{2} = \frac{\int_{ss}\int_{-\pi}^{\pi} \sin^2(\theta-\bar{\theta})E(f,\theta)\mathrm{d}\theta\ \mathrm{d}f}{\int_{ss}\int_{-\pi}^{\pi} E(f,\theta)\mathrm{d}\theta\ \mathrm{d}f}. \quad \text{(A2)}$$

Except for using $\bar{\theta} = \arctan(b_2/a_2)$, the $\bar{\sigma}_\theta^*$ definition is that used by Herbers et al. (1999).

References

Abramowitz, M., Stegun, I., 1965. Handbook of Mathematical Functions Dover, New York.

Battjes, J.A., 1972. Radiation stresses in short-crested waves. J. Mar. Res. 30, 56–64.

Bouws, E., Gunther, H., Rosenthal, W., Vincent, C.L., 1985. Similarity of the wind wave spectrum in finite depth water: I. Spectral form. J. Geophys. Res. 90, 975–986.

Bowen, A.J., Inman, D.L., Simmons, V.P., 1968. Wave "set-down" and set-up. J. Geophys. Res. 73, 2569–2577.

Church, J.C., Thornton, E.B., 1993. Effects of breaking wave induced turbulence within a longshore current model. Coast. Eng. 20, 1–28.

Elgar, S., Herbers, T.H.C., Guza, R.T., 1994. Reflection of ocean surface gravity waves from a natural beach. J. Phys. Oceanogr. 24, 1503–1511.

Guza, R.T., Thornton, E.B., 1981. Wave set-up on a natural beach. J. Geophys. Res. 86, 4133–4137.

Herbers, T.H.C., Elgar, S., Guza, R.T., 1999. Directional spreading of waves in the nearshore. J. Geophys. Res. 104, 7683–7693.

Higgins, A.L., Seymour, R.J., Pawka, S.S., 1981. A compact representation of ocean wave directionality. Appl. Ocean Res. 3, 105–112.

King, B.A., Blackley, M.W.L., Carr, A.P., Hardcastle, P.J., 1990. Observations of wave-induced set-up on a natural beach. J. Geophys. Res. 95, 22289–22297.

Kinsman, B., 1965. Wind Waves: Their Generation and Propagation on the Ocean Surface Prentice-Hall, Englewood Cliffs, NJ. 676 pp.

Kuik, A.J., Van Vledder, G.P., Holthuijsen, L.H., 1988. A method for the routine analysis of pitch-and-roll buoy wave data. J. Phys. Oceanogr. 18, 1020–1034.

Lentz, S.J., Raubenheimer, B., 1999. Field observations of wave setup. J. Geophys. Res. 104, 25867–25875.

Lentz, S.J., Guza, R.T., Elgar, S., Feddersen, F., Herbers, T.H.C., 1999. Momentum balances on the North Carolina inner shelf. J. Geophys. Res. 104, 18205–18226.

Long, C.E., 1996. Index and bulk parameters for frequency-direction spectra measured at CERC Field Research Facility, June 1994 to August 1995, Misc. Pap. CERC-96-6, U.S. Army Eng. Waterw. Exp. Stn., Vicksburg, MS.

Longuet-Higgins, M.S., 1970. Longshore currents generated by obliquely incident sea waves 1. J. Geophys. Res. 75, 6790–6801.

Longuet-Higgins, M.S., Stewart, R.W., 1964. Radiation stress in water waves, a physical discussion with application. Deep-Sea Res. 11, 529–563.

Longuet-Higgins, M.S., Cartwright, D.E., Smith, N.D., 1963. Observations of the directional spectrum of sea waves using the motion of a floating buoy. Ocean Wave Spectra. Prentice-Hall, Englewood Cliffs, NJ, pp. 111–136.

Nielsen, P., 1988. Wave setup: a field study. J. Geophys. Res. 93, 15642–15652.

Pierson, W.J., Moskowitz, L., 1964. A proposed spectral form for fully developed wind seas based on the similarity theory of S.A. Kitaigorodskii. J. Geophys. Res. 69, 5181–5190.

Raubenheimer, B., Guza, R.T., Elgar, S., 2001. Field observations of wave-driven setdown and setup. J. Geophys. Res. 106, 4629–4638.

Ruessink, B.G., Miles, J.R., Feddersen, F., Guza, R.T., Elgar, S., 2001. Modeling the alongshore current on barred beaches. J. Geophys. Res. 106, 22451–22463.

Thornton, E.B., Guza, R.T., 1986. Surf zone longshore currents and random waves: field data and models. J. Phys. Oceanogr. 16, 1165–1178.